

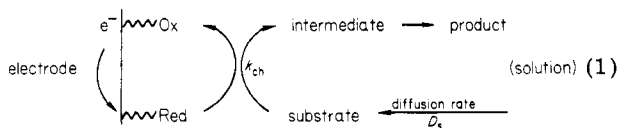
# Kinetics of Electrocatalysis of Dibromoalkyl Reductions Using Electrodes with Covalently Immobilized Metallotetraphenylporphyrins

Roy D. Rocklin and Royce W. Murray\*

Kenan Laboratories of Chemistry, University of North Carolina, Chapel Hill, North Carolina 27514 (Received: December 5, 1980; In Final Form: March 18, 1980)

The reduction of  $\text{PhCHBrCH}_2\text{Br}$ ,  $\text{PhCHBrCHBrPh}$ , and  $\text{CH}_2\text{BrCHBrCH}_3$  at the surfaces of electrodes to which cobalt(II) or copper(II) tetra(*p*-aminophenyl)porphyrin had been covalently attached is strongly catalyzed by reduction of the metalloporphyrin. The rate of the electrocatalytic reduction was measured by using rotated disk electrode voltammetry and was independent of the amount of metalloporphyrin on the electrode above an estimated monomolecular coverage level. The results are consistent with theory which assumes that the rate of diffusion of electrochemical charge through the porphyrin layer is faster than the rate of diffusion of catalytic substrate through the layer. Comparison of the electrocatalytic rates for the different substrates indicates the electron-transfer mediation involves specific interactions between substrate and metalloporphyrin rather than being a simple outer-sphere electron-transfer event. Potential step chronoamperometry is introduced as an alternative method for electrocatalytic measurements at modified electrodes.

There has been great interest over the past several years in bonding or coating monomolecular and multimolecular layers of chemicals on electrode surfaces so as to give the electrode special or distinctive characteristics. A number of chemical and physical preparative routes to such chemically modified electrode surfaces have been described.<sup>1</sup> Increasingly, efforts are being directed toward preparing surfaces which accelerate electrochemical reactions of substances dissolved in the contacting solution which are at naked electrode surfaces only slowly electrochemically oxidized or reduced. Such electrocatalysis normally involves redox transformations of the immobilized chemicals which mediate, in an outer-sphere electron-transfer step or in more complex reaction chemistry, the oxidative or reductive transfer of electrons between the electrode surface and the dissolved substrate. The two electrocatalytic situations have been termed, respectively, redox catalysis and chemical catalysis.<sup>2,3</sup> Mediated electrocatalysis is, for reduction, represented by the general scheme

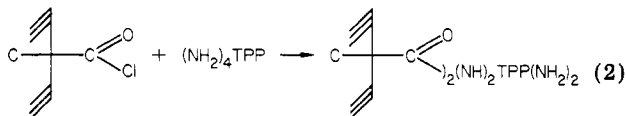


where Ox/Red is the immobilized redox couple of which Red reacts with substrate at rate  $k_{\text{ch}}$  to give a product which is rapidly and irreversibly transformed into another product.

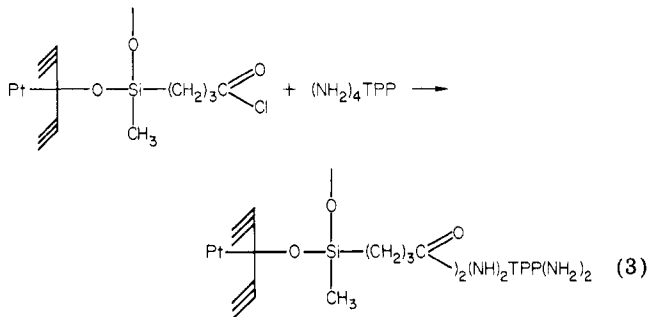
Interesting and imaginative, but qualitative, illustrations of this scheme have been successfully achieved,<sup>4-12</sup> whereas

quantitative electrocatalytic studies and measurements of  $k_{\text{ch}}$  are scarce. Oyama and Anson<sup>6a</sup> have measured  $k_{\text{ch}}$  between dissolved metal complexes and  $\text{IrCl}_6^{3-}$  trapped in an anion-exchange film coated on a rotated carbon disk, and Lewis et al.<sup>5a</sup> have measured  $k_{\text{ch}}$  between ferrocenium photogenerated in a polymer film and iodide in solution. Cyclic voltammetry theory has been presented for reaction 1 but without illustrative experiments.<sup>2</sup>

We have described procedures for immobilizing tetra(*p*-aminophenyl)porphyrin ( $\text{NH}_2$ )<sub>4</sub>TPP by reacting it with thionyl chloride-treated glassy carbon<sup>11a,13</sup>



and with superficially oxidized, silanized  $\text{Pt}^{14}$



- (1) Murray, R. W. *Acc. Chem. Res.* 1980, 13, 135.  
 (2) Andrieux, C. P.; Saveant, J. M. *J. Electroanal. Chem.* 1978, 93, 163.  
 (3) Electrocatalysis, conceptually, can also be based on surface mediation of proton, ligand, or metal ion transfers.  
 (4) (a) Evans, J. F.; Kuwana, T.; Henne, M. T.; Royer, G. P. *J. Electroanal. Chem.* 1977, 80, 409. (b) Tse, D. C. S.; Kuwana, T. *Anal. Chem.* 1978, 50, 1315. (c) Bettelheim, A.; Chan, R. J. H.; Kuwana, T. *J. Electroanal. Chem.* 1979, 99, 391.  
 (5) (a) Lewis, N. S.; Bocarsly, A. B.; Wrighton, M. S. *J. Phys. Chem.* 1980, 84, 2033. (b) Bolts, J. M.; Bocarsly, A. B.; Palazzotto, M. C.; Walton, E. G.; Lewis, N. S.; Wrighton, M. S. *J. Am. Chem. Soc.* 1979, 101, 1378. (c) Bocarsly, A. B.; Walton, E. G.; Bradley, M. G.; Wrighton, M. S. *J. Electroanal. Chem.* 1979, 100, 283. (d) Bocarsly, A. B.; Walton, E. G.; Wrighton, M. S. *J. Am. Chem. Soc.* 1980, 102, 3390.  
 (6) (a) Oyama, N.; Anson, F. C. *Anal. Chem.* 1980, 52, 1192. (b) Anson, F. C. *J. Phys. Chem.* 1980, 84, 3336.

- (7) (a) Collman, J. P.; Marrocco, M.; Denisevich, P.; Koval, C.; Anson, F. C. *J. Electroanal. Chem.* 1979, 101, 117. (b) Collman, J. P.; Denisevich, P.; Konai, Y.; Marrocco, M.; Koval, C.; Anson, F. C. *J. Am. Chem. Soc.* 1980, 102, 6027.  
 (8) Zagal, J.; Sen, R. K.; Yeager, E. *J. Electroanal. Chem.* 1977, 83, 207.  
 (9) (a) Kerr, J. B.; Miller, L. L.; Van De Mark, M. R. *J. Electroanal. Chem.* 1979, 101, 263. (b) Miller, L. L.; Van De Mark, M. R. *J. Am. Chem. Soc.* 1978, 100, 3223. (c) Kerr, J. P.; Van De Mark, M. R.; Miller, L. L. *Ibid.* 1980, 102, 3383. (d) Degrand, C.; Miller, L. L. *Ibid.* 1980, 102, 5728.  
 (10) Stargardt, J. F.; Hawkrigde, F. M.; Landrum, H. L. *Anal. Chem.* 1978, 50, 930.  
 (11) (a) Rocklin, R. D.; Murray, R. W. *J. Electroanal. Chem.* 1979, 100, 271. (b) Denisevich, P.; Abruña, H. D.; Umaña, M.; Meyer, T. J.; Murray, R. W. *J. Am. Chem. Soc.* 1981, 103, 1. (c) Abruña, H. D.; Walsh, J. L.; Meyer, T. J.; Murray, R. W. *Ibid.* 1980, 102, 3272.  
 (12) (a) Dautartas, M. F.; Mann, K. R.; Evans, J. F. *J. Electroanal. Chem.* 1980, 110, 379. (b) Dautartas, M. F.; Evans, J. F. *Ibid.* 1980, 109, 301.

Two surface amide bonds (on the average) are formed in reactions 2 and 3,<sup>13c,14a</sup> the products of which we abbreviate, respectively, as C/ $\sim$ (NH<sub>2</sub>)<sub>4</sub>TPP and Pt/ $\sim$ (NH<sub>2</sub>)<sub>4</sub>TPP, and which can be subsequently metallated, to C/ $\sim$ (M)-(NH<sub>2</sub>)<sub>4</sub>TPP and Pt/ $\sim$ (M)(NH<sub>2</sub>)<sub>4</sub>TPP, where M = Co, Cu, Zn, and Mn<sup>11a</sup> among others.

These porphyrin electrode surfaces have proven to be electrocatalytically active toward reduction of alkyl bromides which are classically slowly reduced at naked electrodes.<sup>16</sup> The electrocatalytic activity is rapidly degraded during reductions of monobromo species, but several 1,2-dibromoalkyl substrates exhibited sufficient stability for quantitative kinetic studies, which were undertaken. We report here measurements of catalytic rate as a function of substrate, of metal, and of porphyrin coverage as attained in reaction 3 from submonomolecular to multimolecular. Most of the rate measurements were performed with rotated disk electrode voltammetry; in the interests of testing new methodology some were carried out with potential step chronoamperometry. The dibromo substrates used are 1,2-dibromo-1,2-diphenylethane (PhCHBrCHBrPh), 1,2-dibromophenylethane (PhCHBrCH<sub>2</sub>Br), and 1,2-dibromopropane (CH<sub>2</sub>BrCHBrCH<sub>3</sub>). The results for reduction of PhCHBrCH<sub>2</sub>Br show that the catalytically reactive zone on Pt/ $\sim$ (Co)-(NH<sub>2</sub>)<sub>4</sub>TPP and Pt/ $\sim$ (Cu)(NH<sub>2</sub>)<sub>4</sub>TPP electrodes is the outermost layer of porphyrin sites.

### Experimental Section

**Chemicals.** *meso*-Tetra(*p*-aminophenyl)porphyrin, (NH<sub>2</sub>)<sub>4</sub>TPP, was synthesized by the Adler method,<sup>15</sup> refluxing equimolar amounts of pyrrole and *p*-acetamidobenzaldehyde (ca. 5 g) in 250 mL of propionic acid for 30 min, then adding 250 mL of concentrated HCl to the cooled solution, and refluxing again to hydrolyze the acetyl grouping. Cooling the solution in an ice bath and neutralizing with aqueous ammonia gives a brown precipitate which was filtered, air dried, and extracted with tetrahydrofuran. The extract was concentrated to 50 mL and 500 mL of diethyl ether was added, precipitating impurities. The deep red solution was filtered, concentrated, and chromatographed on a silica gel column with 95% CH<sub>2</sub>Cl<sub>2</sub>/5% CH<sub>3</sub>OH; taking the central band fraction to dryness and extracting with CH<sub>2</sub>Cl<sub>2</sub> was followed by final chromatography on a short silica gel column with 99% CH<sub>2</sub>Cl<sub>2</sub>/1% CH<sub>3</sub>OH.

PhCHBrCH<sub>2</sub>Br was recrystallized twice from 2-propanol and PhCHBrCHBrPh once from acetone. CH<sub>2</sub>BrCHBrCH<sub>3</sub> was washed with concentrated H<sub>2</sub>SO<sub>4</sub>, neutralized with Na<sub>2</sub>CO<sub>3</sub>, washed with water, dried with MgSO<sub>4</sub>, and fractionally distilled. The electrochemical solvent dimethyl sulfoxide, Me<sub>2</sub>SO, was dried over Linde 4 Å molecular sieves and contained 0.1 M tetraethylammonium perchlorate supporting electrolyte.

**Electrodes.** Glassy carbon electrodes were polished on the cylinder ends (0.06 cm<sup>2</sup>), finishing with 1- $\mu$ m diamond paste. The porphyrin was attached by refluxing the electrodes with 1–2 mL of freshly distilled thionyl chloride in 15 mL of Na<sup>0</sup> dried toluene, briefly rinsing, then 2-h exposure to a refluxing solution of ca. 1 mg of porphyrin in 15 mL of toluene. The metals were inserted in refluxing

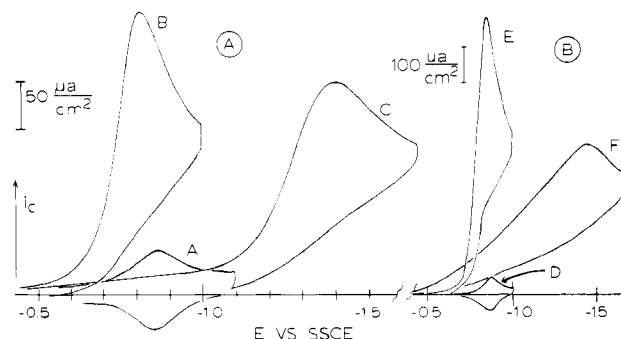


**Figure 1.** Cyclic voltammetry. Panel A: Electrocatalytic reduction of 1 mM PhCHBrCH<sub>2</sub>Br by C/ $\sim$ (Co)(NH<sub>2</sub>)<sub>4</sub>TPP in Me<sub>2</sub>SO/0.1 M TEAP, 100 mV/s, SSCE reference, 25 °C; curve A, porphyrin surface, no substrate,  $\Gamma_T = 4.2 \times 10^{-10}$  mol/cm<sup>2</sup>; curve B, catalyzed reduction; curve C reduction of substrate on naked glassy carbon.  $E_{p,uncat} = -1.40$  V. Panel B: Electrocatalytic reduction of 2.62 mM PhCHBrCH<sub>2</sub>Br by Pt/ $\sim$ (Co)(NH<sub>2</sub>)<sub>4</sub>TPP in Me<sub>2</sub>SO/0.1 M TEAP, 100 mV/s, SSCE reference, 25 °C; curve D, porphyrin surface,  $\Gamma_T = 5.45 \times 10^{-10}$  mol/cm<sup>2</sup>; curve E, catalyzed reduction; curve F, reduction of substrate on naked Pt electrode,  $E_{p,uncat} = -1.44$  V. Comparison of the foot of curves E and F shows that direct substrate reduction at the modified electrode is blocked by the catalyst film.

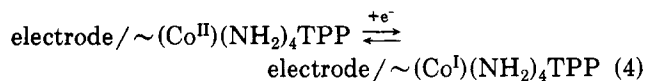
DMF solutions of the metal(II) chloride for 15 min followed by washing in DMF and CH<sub>3</sub>OH, air drying, and mounting on a brass holder with heat-shrink Teflon.

One micron diamond paste polished Pt disks (0.1 cm<sup>2</sup>), Teflon shrouded, were modified by placing a drop of neat 4-methyldichlorosilylbutryl chloride on the surface in room air for 1 min, briefly rinsing in toluene, and exposure to a hot toluene solution (5 mL) containing ca. 1 mg of porphyrin. The porphyrin surface was metallated with cobalt by warming the electrode to either 75 or 90 °C for 6 h in a DMF solution of CoCl<sub>2</sub>. Copper was inserted by warming the silanized electrode to ca. 50 °C in a DMF solution of CuCl<sub>2</sub> for 1 h.

**Electrochemical Experiments.** Electrochemical equipment and cells were of conventional design. Prior to measurement of electrocatalytic currents the porphyrin-coated electrode was inspected with cyclic voltammetry to measure the porphyrin coverage from its electrochemical wave. Rotated disk experiments were conducted with a Pine Instruments rotator, and limiting current values were typically taken at a fixed potential on the catalytic wave plateau. Electrode potentials are referenced to a NaCl saturated SCE (SSCE).

### Results and Discussion

**Cyclic Voltammetry.** Cyclic voltammetry is a useful qualitative tool to ascertain the existence and stability of catalysis for a given metalloporphyrin–substrate combination. Results with C/ $\sim$ (Co)(NH<sub>2</sub>)<sub>4</sub>TPP and Pt/ $\sim$ (Co)(NH<sub>2</sub>)<sub>4</sub>TPP surfaces and PhCHBrCH<sub>2</sub>Br substrate are shown in Figure 1. The immobilized metalloporphyrin wave, corresponding to the reaction ( $E_{surf}^{0'} = -0.86$  V vs. SSCE) (curves A and D)



is determined in the absence of substrate to assess the total coverage of porphyrin on the electrode,  $\Gamma_T$ , and additionally, after electrocatalysis experiments, to inspect for surface degradation. Quantitative kinetic data are reported here only when the electrode degradation has been minimal (<20% change).

In the absence of immobilized porphyrin, Figure 1, curves C and F, shows that PhCHBrCH<sub>2</sub>Br is reduced on

(13) (a) Lennox, J. C.; Murray, R. W. *J. Electroanal. Chem.* 1977, 78, 395. (b) Jester, C. P.; Rocklin, R. D.; Murray, R. W. *Ibid.* 1980, 127, 1979. (c) Lennox, J. C.; Murray, R. W. *J. Am. Chem. Soc.* 1978, 100, 3710.

(14) (a) Willman, K. W.; Rocklin, R. D.; Nowak, R.; Kuo, K.; Schultz, F. A.; Murray, R. W. *J. Am. Chem. Soc.* 1980, 102, 7629. (b) Smith, D. F.; Willman, K.; Kuo, K.; Murray, R. W. *J. Electroanal. Chem.* 1979, 95, 217.

(15) Adler, A. D.; Longo, F. R.; Finarelli, J. D.; Goldmacher, J.; Assour, J.; Korsakoff, J. *J. Org. Chem.* 1967, 32, 476.

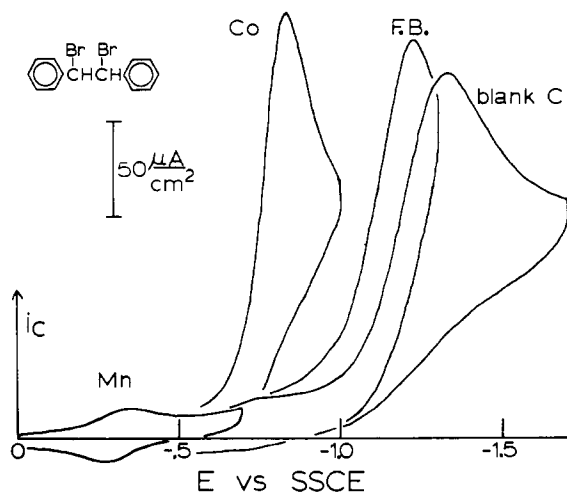
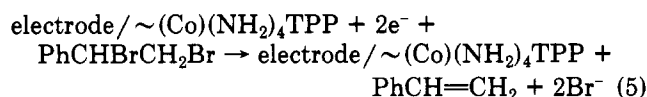


**Figure 2.** Cyclic voltammetry of 1 mM PhCHBrCHBrPh at C/(M)-(NH<sub>2</sub>)<sub>4</sub>TPP in Me<sub>2</sub>SO/0.1 M TEAP, 100 mV/s, SSCE reference, 25 °C.  $\Gamma_T(\text{Mn}) = 1.7 \times 10^{-10}$  mol/cm<sup>2</sup>,  $\Gamma_T(\text{Co}) = 2.5 \times 10^{-10}$ ,  $\Gamma_T(\text{NH}_2)_4\text{TPP}$  (free base) =  $3.9 \times 10^{-10}$ , all curves except "blank C" contain both substrate and porphyrin layer.

naked glassy carbon and Pt in a drawn out wave at ca. -1.4 V vs. SSCE. Significantly, silanization of the Pt causes little change in curve F. Using electrodes to which cobalt-metallated porphyrin has been attached causes a strong voltage catalysis, shifting the PhCHBrCH<sub>2</sub>Br reduction by 560–600 mV, curves B and E. Judging from the relative heights of the catalyzed and uncatalyzed waves in Figure 1, and the absence of any anodic wave for reaction 4 in the presence of PhCHBrCH<sub>2</sub>Br, we feel the catalysis is fast, occurring at or near a diffusion-controlled rate. The catalyzed reaction occurs near the potential for reaction 4, as expected if the reduced form of the porphyrin acts to transfer electrons to the substrate. Reductions of 1,2-dibromoalkyls are known<sup>16,17</sup> to yield olefins, and Miller<sup>9a,b</sup> has demonstrated that the electrocatalytic reduction of PhCHBrCH<sub>2</sub>Br by a poly(*p*-nitrostyrene) film on an electrode yields styrene as product. These porphyrin surfaces are, however, not sufficiently stable for product analysis studies, and so we assume by analogy with the earlier work that the electrochemical reaction in Figure 1 has the stoichiometry



Reduction of PhCHBrCH<sub>2</sub>Br is also catalyzed by a porphyrin surface which has been metallated with Cu, giving a current peak near  $E_{\text{surf}}^{\circ'}$  for this metalloporphyrin, -1.21 V, and by porphyrin surfaces which have not been metallated at all. In the latter, free base porphyrin catalysis, in contrast to the Co and Cu examples, the electrocatalytic effect persists only for a small number of cyclical potential scans, making quantitative experiments impossible. The Co and Cu porphyrin electrodes are sufficiently stable for quantitative rotated disk and chronoamperometric kinetic studies.

Results for reduction of PhCHBrCHBrPh and CH<sub>2</sub>BrCHBrCH<sub>3</sub> are given in Figures 2 and 3. For PhCHBrCHBrPh, electrocatalysis occurs with the free base (again unstable) and cobalt-metallated porphyrin, whereas manganese porphyrin is ineffective. For CH<sub>2</sub>-

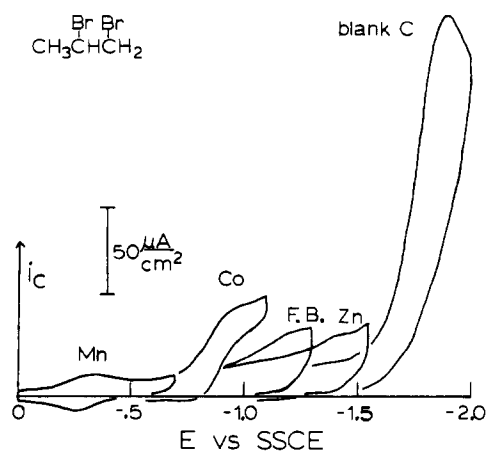


**Figure 3.** Cyclic voltammetry of 1 mM CH<sub>3</sub>CHBrCH<sub>2</sub>Br at C/(M)-(NH<sub>2</sub>)<sub>4</sub>TPP in Me<sub>2</sub>SO/0.1 M TEAP, 100 mV/s, SSCE reference, 25 °C.  $\Gamma_T(\text{Mn}) = 1.7 \times 10^{-10}$  mol/cm<sup>2</sup>,  $\Gamma_T(\text{Co}) = 2.5 \times 10^{-10}$ ,  $\Gamma_T(\text{free base}) = 1.0 \times 10^{-10}$ ,  $\Gamma_T(\text{Zn}) = 8 \times 10^{-11}$ , all curves except "blank C" contain both substrate and porphyrin layer.

**TABLE I: Cyclic Voltammetric Estimates<sup>b</sup> of Alkyl Dibromide Electrocatalysis in Me<sub>2</sub>SO**

porphyrin, <sup>a</sup> $E_{\text{surf}}^{\circ'}$	substrate, $E_{p,\text{uncat}}$		
	PhCHBr- CHBrPh, -1.32	PhCHBr- CH <sub>2</sub> Br, -1.40	CH <sub>2</sub> CHBr- CH <sub>2</sub> Br, -1.89
Mn, -0.30	no	no	no
Co, -0.87	fast	fast	slow
free base, -1.12	fast <sup>c</sup>	fast <sup>c</sup>	no
Cu, -1.21	<i>d</i>	fast	no
Zn, -1.42	<i>d</i>	<i>d</i>	no

<sup>a</sup> Immobilized on glassy carbon electrode by reaction 2. Potentials referenced to NaCl saturated SCE. <sup>b</sup> Fast means approximately diffusion controlled;  $i_p/v^{1/2} \sim \text{constant}$  at  $v \leq 50$  mV/s. <sup>c</sup> Reacts with substrate. <sup>d</sup> Excessive overlap with the uncatalyzed reduction.

BrCHBrCH<sub>3</sub>, reduced at a rather negative potential on naked Pt, only the cobalt porphyrin shows any activity. The mechanistic implication of these results, summarized in Table I, is considered later.

**Rotated Disk Voltammetry. Limiting Current Theory.** For this technique, the published relationship is<sup>6,18</sup>

$$\frac{1}{i_{\text{max}}} = \frac{1}{nFAk_{\text{ch}}\Gamma C_S} + \frac{1}{0.62nFAD_S^{2/3}\nu^{-1/6}\omega^{1/2}C_S} \quad (6)$$

where  $i_{\text{max}}$  is the limiting current of the electrocatalyzed wave,  $k_{\text{ch}}$  (cm<sup>3</sup>/mol s) is the rate constant for the reaction of substrate (concentration  $C_S$ , mol/cm<sup>3</sup>) with reduced porphyrin sites according to the rate law  $-d\Gamma/dt = k_{\text{ch}}\Gamma C_S$ ,  $D_S$  is the diffusion coefficient of substrate in the solution, and  $\omega$  is the rate of electrode rotation in rad/s. This equation predicts that at the  $1/\omega^{1/2} = 0$  intercept of a  $1/i_{\text{max}}$  vs.  $1/\omega^{1/2}$  plot, called a Koutecky-Levich plot,<sup>18</sup> the current is limited solely by the rate of substrate-reduced porphyrin chemical reaction and not by the mass transport of substrate from the solution to the rotated electrode. Equation 6 has been applied by Oyama and Anson<sup>6a</sup> and by Alberly et al.<sup>19</sup> in modified electrode studies.

By manipulating the conditions of Pt electrode silanization preceding reaction 3 so as to produce a siloxane polymer film with reactive acid chloride sites, we found

(16) Rifi, M. R. In "Organic Electrochemistry"; Bazier, M. M.; Ed.; Marcel Dekker: New York, 1973; Chapter VI.

(17) Lund, H.; Hobolth, E. *Acta Chim. Scand.* 1976, B30, 895.

(18) Levich, V. G. "Physicochemical Hydrodynamics"; Prentice-Hall, Englewood Cliffs, NJ, 1962.

(19) Alberly, W. J.; Bowen, W. R.; Foulds, A. W.; Hall, K. J.; Hillman, A. R.; Egdell, R. G.; Orchard, A. F. *J. Electroanal. Chem.* 1980, 107, 37.

it possible to increase the coverage of porphyrin catalyst sites bound via reaction 3 above a monomolecular and submonomolecular level to as much as ca.  $2 \times 10^{-9}$  mol/cm<sup>2</sup>. For electrocatalysis on electrodes covered with polymeric, multimolecular layer films, eq 6 neglects two additional reaction steps. In one, reduced porphyrin catalyst sites migrate outward from the electrode through the polymer film toward incoming substrate, by electron self-exchange<sup>20,21</sup> between neighboring oxidized and reduced porphyrin sites. There is now strong evidence<sup>20,22-25</sup>, despite suggestions to the contrary,<sup>9d</sup> that the rate of this migration of electrochemical charge can be expressed as a Fickian charge-transport process with diffusion constant  $D_{ct}$  (cm<sup>2</sup>/s). The second reaction step is the diffusion of substrate through the polymer film toward reduced porphyrin sites, expressed by the rate  $D_{S,pol}$  in cm<sup>2</sup>/s. Thus, three reaction steps, charge transport, substrate diffusion, and the chemical reaction, occur within the polymer film and may influence the value of  $1/i_{max}$  at  $1/\omega^{1/2} = 0$ .

Theory accounting for all these reaction steps is not yet available. Andrieux and Saveant<sup>2,26</sup> considered cyclic voltammetric current limitation due to diffusion of substrate in a multilayer film, concluding that (under specified conditions) current was controlled by substrate reacting, more or less uniformly, with all catalyst sites in the film (i.e.,  $\Gamma = \Gamma_T$ ). Anson,<sup>6b</sup> considering charge transport and (outer-sphere) chemical rates, concluded that in most cases charge transport was unlikely to control the current, and again that  $\Gamma = \Gamma_T$ . These studies omitted consideration of the third factor of charge transport and substrate diffusion, respectively. In several experimental studies of electrocatalysis,<sup>6a,9d</sup> including this one, however, the apparent chemical reaction rate was not proportional to  $\Gamma_T$ , an effect not accounted for by these theories, but which can be explained by elementary theory which follows.

Consider<sup>27</sup> the three reaction steps in terms of their flux (mol/cm<sup>2</sup> s) when current-controlling, (CT flux)<sub>lim</sub>, (CHEM flux)<sub>lim</sub>, and (SUBS flux)<sub>lim</sub>, and when one of the other steps dominates, CT flux, CHEM flux, and SUBS flux, all at the  $1/\omega^{1/2} = 0$  intercept. The current is necessarily equated to the steady-state flux of reduced catalyst sites, i.e., the charge transport rate

$$\frac{i_{max}}{nFA} = CT \text{ flux} = \frac{D_{ct}[C_{TPP(x=0)} - C_{TPP(x=p)}]}{p} \quad (7)$$

where  $C_{TPP}$  is the concentration of reduced porphyrin catalyst sites (at  $x = 0$ ,  $C_{TPP} = \Gamma_T/d$ , where  $d$  is film thickness) and  $p \leq d$  is a distance interval in the film over which a  $C_{TPP}$  gradient exists. If  $i_{max}$  is controlled by the charge transport rate, eq 7 becomes

$$(CT \text{ flux})_{lim} = \frac{D_{ct}C_{TPP(x=0)}}{d} = \frac{D_{ct}\Gamma_T}{d^2} \quad (8)$$

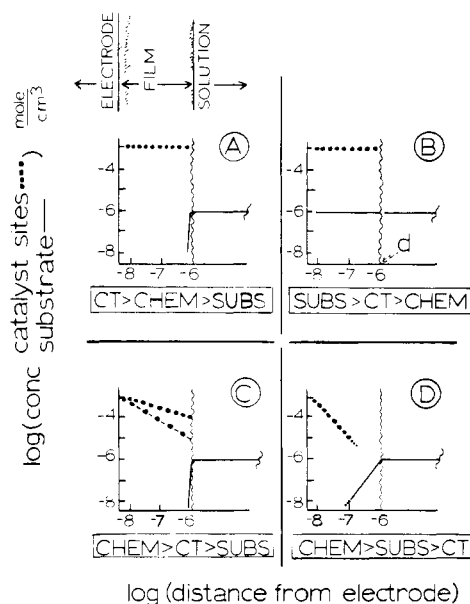


**Figure 4.** Estimated steady-state concentration distance profiles of catalyst sites (CAT, ●) and substrate (SUBS, —) for electrocatalysis at rotated disk electrode, at the  $1/\omega^{1/2} = 0$  intercept of a  $1/i_{max}$  vs.  $1/\omega^{1/2}$  plot, assuming  $C_S = 1 \times 10^{-6}$  mol/cm<sup>3</sup>,  $\Gamma_T = 1 \times 10^{-9}$  mol/cm<sup>2</sup>,  $d = 1 \times 10^{-6}$  cm,  $C_{TPP(x=0)} = 1 \times 10^{-3}$  mol/cm<sup>3</sup>, flux values all in mol/cm<sup>2</sup> s. Panel A: (CHEM flux)<sub>lim</sub> =  $1 \times 10^{-8}$  mol/cm<sup>2</sup> s, CT flux =  $4 \times 10^{-7}$  ( $D_{ct} = 4 \times 10^{-10}$  cm<sup>2</sup>/s), SUBS flux =  $1 \times 10^{-9}$  ( $D_{S,pol}P = 1 \times 10^{-9}$  cm<sup>2</sup>/s),  $k_{ch}\Gamma_C S = 1 \times 10^{-8}$ . Panel B: (CHEM flux)<sub>lim</sub> =  $1 \times 10^{-8}$  mol/cm<sup>2</sup> s, CT flux =  $4 \times 10^{-7}$  ( $D_{ct} = 4 \times 10^{-10}$  cm<sup>2</sup>/s), SUBS flux =  $1 \times 10^{-9}$  ( $D_{S,pol}P = 1 \times 10^{-9}$  cm<sup>2</sup>/s),  $k_{ch}\Gamma_C S = 1 \times 10^{-8}$ . Panel C: (CT flux)<sub>lim</sub> =  $4 \times 10^{-7}$  mol/cm<sup>2</sup> s ( $D_{ct} = 4 \times 10^{-10}$  cm<sup>2</sup>/s), CHEM flux  $> 4 \times 10^{-6}$  (●—●—●),  $4 \times 10^{-5}$  (●●●●), SUBS flux =  $1 \times 10^{-9}$  ( $D_{S,pol}P = 1 \times 10^{-9}$  cm<sup>2</sup>/s). Panel D: (SUBS flux)<sub>lim</sub> =  $1 \times 10^{-9}$  ( $D_{S,pol}P = 1 \times 10^{-9}$  cm<sup>2</sup>/s), CHEM flux =  $1 \times 10^{-8}$  ( $C_{TPP(x=10^{-7})} = 0.01C_{TPP(x=0)}$ ;  $C_{S(x=10^{-7})} = 0.01C_{S(x=d)}$ ), CT flux =  $1 \times 10^{-7}$  ( $D_{ct} = 1 \times 10^{-12}$  cm<sup>2</sup>/s,  $p = 1 \times 10^{-7}$  cm).

The flux of substrate consumed by the chemical reaction CHEM flux, is equal to CT flux, and if it is limiting

$$(CHEM \text{ flux})_{lim} = k_{ch}\Gamma_C S \quad (9)$$

and eq 6 results. Note that, in eq 6 and 9,  $\Gamma$  is the coverage of catalyst sites which actually undergo reaction with substrate and is not presumed equal to  $\Gamma_T$ .

The flux of substrate SUBS flux diffusing into the polymer film to be consumed by catalyst sites must be equal to both CHEM flux and CT flux and is given by

$$SUBS \text{ flux} = \frac{D_{S,pol}P[C_S(x=d) - C_S(x=q)]}{d - q} \quad (10)$$

where  $C_{S(x)}$  is the concentration of substrate in the polymer film forming a gradient over the distance interval  $d - q$ , and  $P$  is the partition coefficient with which substrate dissolves into the polymer film from the solution. The product  $D_{S,pol}P$  can be small, especially if entrance of substrate into the polymer film is made unfavorable by substrate charge (ion exchange film co-ion exclusion) or molecular size considerations. It is physically reasonable, however, to assume that the electrocatalysis can proceed even if  $D_{S,pol}P$  is very small, since substrate need not diffuse within the polymer film to react with catalyst sites accessible at the polymer/solution interface.

Keeping in mind that one of the reaction fluxes can limit the others, which can force  $p < d$  in eq 7 and  $d - q < d$  in eq 10, we can employ the flux relationships to estimate steady-state concentration distance profiles within polymer films on rotated disk electrodes. Six limiting conditions are conceivable according to the ordering of the three fluxes; four are shown in the diagrams of Figure 4. A fifth

(20) Daum, P.; Lenhard, J. R.; Rolison, D. R.; Murray, R. W. *J. Am. Chem. Soc.* 1980, 102, 4649.

(21) (a) Kaufman, F. B.; Engler, E. M., *J. Am. Chem. Soc.* 1979, 101, 547. (b) Kaufman, F. B.; Schroeder, A. H.; Engler, E. M. *Chambers, J. Q.*; *Ibid.* 1980, 102, 483.

(22) Daum, P.; Murray, R. W. *J. Phys. Chem.* 1981, 85, 389.

(23) Oyama, N.; Anson, F. C. *J. Electrochem. Soc.* 1980, 127, 640.

(24) Pearce, P. J.; Bard, A. J., *J. Electroanal. Chem.* 1980, 114, 89.

(25) Nowak, R. J.; Schultz, E. A.; Umana, M.; Lam, R.; Murray, R. W. *Anal. Chem.* 1980, 52, 315.

(26) Andrieux, C. P.; Dumas-Bouchiat, J. M.; Saveant, J. M. *J. Electroanal. Chem.* 1980, 114, 159.

(27) Assume that the rate of nonmediated reaction of substrate at the electrode surface is negligibly slow, that electron transfer to porphyrin at the electrode/polymer interface is fast, and that the kinetics of dissolution of substrate into the polymer film from the solution are fast.

condition, SUBS > CT > CHEM flux, is like panel B. The parameters chosen to estimate these diagrams,  $D_{ct} = 10^{-12}$  to  $4 \times 10^{-10}$  cm<sup>2</sup>/s,  $D_{S,pol} = 10^{-6}$  to  $10^{-9}$  cm<sup>2</sup>/s, and  $k_{ch}\Gamma_{CS} = 10^{-4}$  to  $10^{-8}$  mol/cm<sup>2</sup>s (corresponding to  $10^3 k_{ch} = 10^4$  to  $10^8$  L/mol s) have values reasonably expectable under various circumstances of polymer film structure and reactivity, and lie within or near the values chosen by Anson<sup>6b</sup> (except for  $D_{S,pol}P$  which Anson did not examine). The values of limiting flux furthermore all lie within or near those measurable<sup>6b</sup> at useful values of  $\omega$  ( $10$ – $10^3$  rad/s) of the rotated disk electrode. The instructive aspect of Figure 4, in panels A, C, and D, is that the zone of catalytic sites where substrate is consumed can become quite narrow so that  $\Gamma \ll \Gamma_T$ . Only when  $D_{S,pol}P$  is large (panel B) or CHEM flux is small, do catalyst sites throughout the film participate in the reaction with substrate so that  $\Gamma \sim \Gamma_T$ . The diagrams in Figure 4 illustrate the necessity of considering three rather than two reaction steps to appreciate the potential range of electrocatalytic behavior of electrodes coated with multimolecular layers of catalyst sites.

The diagrams in Figure 4 furthermore suggest a reformulation of the  $1/\omega^{1/2}$  intercept term of eq 6. In an impedance sense, comparison of panels A, B, and C in particular suggest that the charge transport and substrate diffusion steps can be expressed as elements which are in parallel with one another, this parallel combination being in series with the chemical step, which yields the revised intercept term

$$\frac{1}{nFAk_{ch}\Gamma_{CS}} + \frac{1}{nFAD_{S,pol}PC_{S(x=d)}/d + nFAD_{ct}\Gamma_T/d^2} \quad (11)$$

This relationship is approximate in several respects, but nonetheless can serve to anticipate functional dependences on  $C_S$ ,  $d$ , etc., to detect various forms of rate control of electrocatalytic currents by one or a combination of the three reaction steps discussed above. In limiting forms, eq 11 represents panels A, B, and C, and panel D approximately, in Figure 4, and we have preliminarily discussed some of these limits.<sup>22</sup>

*The Rising Part of the Rotated Disk Electrocatalytic Wave.* If we assume that the chemical reaction flux is the controlling reaction step (i.e., eq 6), and that the porphyrin sites on the electrode surface are, activity wise, noninteracting so that the potential dependency of reduced porphyrin sites is

$$E = E'_{surf} + \frac{RT}{nF} \ln \frac{\Gamma_T - \Gamma_R}{\Gamma_R} \quad (12)$$

where  $E'_{surf}$  is the formal potential of the porphyrin surface wave and  $\Gamma_R$  is coverage of reduced sites, than the catalytic wave equation resulting is

$$E = E'_{surf} + \frac{RT}{nF} \ln \left[ 1 + \frac{k_{ch}\Gamma}{0.62D_S^{2/3}\nu^{-1/6}\omega^{1/2}} \right] + \frac{RT}{nF} \ln \left[ \frac{i_{max} - i}{i} \right] \quad (13)$$

Equation 13 predicts the shape of the electrocatalytic wave (plot  $E$  vs.  $\ln [(i_{max} - i)/i]$ ) and that  $k_{ch}\Gamma$  can be obtained from  $E_{1/2}$ . The difficulty with eq 13, as we shall see, is that the population of reduced porphyrin sites increases more gradually with potential than given by eq 12, as is typical of electrode immobilized chemicals.<sup>1</sup>

*Rotated Disk Electrode Voltammetry, Kinetic Measurements.* The electrocatalytic reduction of PhCHBrCH<sub>2</sub>Br using a Pt/(Cu)(NH<sub>2</sub>)<sub>4</sub>TPP surface is

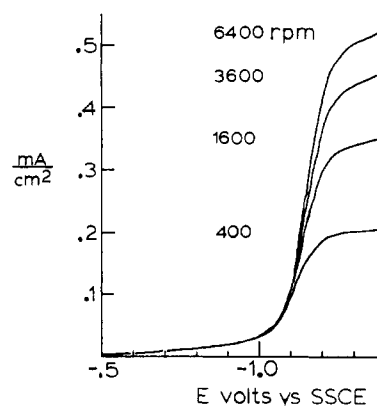


Figure 5. Rotated disk voltammetry for the reduction of 0.69 mM PhCHBrCH<sub>2</sub>Br at a Pt/(Cu)(NH<sub>2</sub>)<sub>4</sub>TPP electrode ( $\Gamma_T = 4.1 \times 10^{-10}$  mol/cm<sup>2</sup>), Me<sub>2</sub>SO–0.1 M TEAP, SSCE reference, 10 mV/s sweep rate, 20 °C. This electrode is entry 1 in Table II.

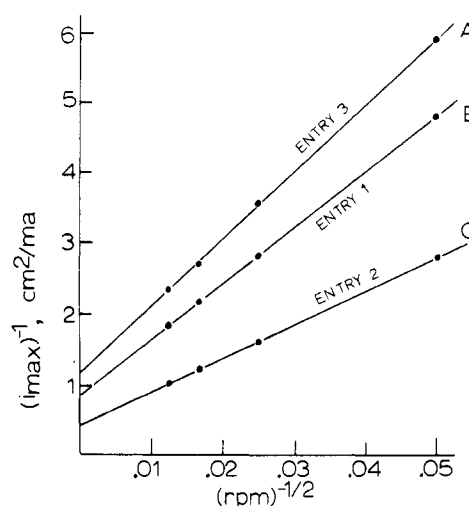


Figure 6. Plot of  $i_{max}^{-1}$  vs.  $\omega^{-1/2}$  according to eq 6 for data of Figure 5 (entry 1, Table II) and of entries 2 and 3, Table II. The intercepts are inversely proportional to the concentration of PhCHBrCH<sub>2</sub>Br (see  $k_{ch}\Gamma$  in Table II). The slopes are also inversely proportional to concentration; the ratio of slope to  $C_S$  for the curves A, B, and C is 4.9, 5.5, and 5.4.

shown in Figure 5. Measuring  $i_{max}$  at constant potential (–1.3 V vs. SSCE) to ensure steady state conditions gives the  $i_{max}$  data compared to  $\omega$ , according to eq 6, in Figure 6. The nonzero intercept of Figure 6 shows the PhCHBrCH<sub>2</sub>Br reduction is not mass transfer controlled, but is limited by the kinetics of the electrocatalytic process. Also shown in Figure 6 are results at other substrate concentrations  $C_S$ , which show that the slope and intercept of these Koutecky–Levich plots are inversely proportional to [PhCHBrCH<sub>2</sub>Br] as expected from eq 6 and 11 if charge transport through the porphyrin film is not rate limiting. The slope of curve B, Figure 6, yields  $D_S = 3.5 \times 10^{-6}$  cm<sup>2</sup>/s which agrees with a direct chronoamperometric (Cottrell plot) measurement of  $D_S = 3.5 \times 10^{-6}$  cm<sup>2</sup>/s on a naked Pt electrode using a potential step to –1.65 V (diffusion controlled for the uncatalyzed reaction).

Data taken from the intercepts of plots like Figure 6 (entries 1–3) and others taken at different temperatures are collected in Table II, expressing the intercept as  $k_{ch}\Gamma$  by use of eq 6. A striking aspect of these data is that  $k_{ch}\Gamma$  is not proportional to the total coverage of porphyrin  $\Gamma_T$  but in fact seems independent of it. Note the greater than fourfold changes in  $\Gamma_T$  in entries 1–3 and in 4–7 where  $k_{ch}\Gamma$  varies only by small amounts. On electrodes prepared by reaction 3, we have shown elsewhere that the immobilized

TABLE II: Electrocatalysis Kinetics<sup>a</sup> from Rotated Disk Voltammetry for Reduction of PhCHBrCH<sub>2</sub>Br by Pt/~(Cu)(NH<sub>2</sub>)<sub>4</sub>TPP in Me<sub>2</sub>SO

entry	T, °C	Γ <sub>T</sub> , mol/cm <sup>2</sup>	C <sub>S</sub> , mM	k <sub>ch</sub> Γ, <sup>b</sup> cm/s
1	20	4.1 × 10 <sup>-10</sup>	0.69	0.0089
2	20	5.9 × 10 <sup>-10</sup>	1.16	0.010
3	20	19 × 10 <sup>-10</sup>	0.49	0.0094
4	25	2.3 × 10 <sup>-10</sup>	0.62	0.011
5	25	5.8 × 10 <sup>-10</sup>	0.68	0.011
6	25	8.3 × 10 <sup>-10</sup>	0.48	0.014
7	25	10.5 × 10 <sup>-10</sup>	0.66	0.013
8	30	5.9 × 10 <sup>-10</sup>	1.16	0.015
9	40	5.9 × 10 <sup>-10</sup>	1.16	0.019
10	50	5.9 × 10 <sup>-10</sup>	1.16	0.024

<sup>a</sup> A value of  $n = 2$  is used in calculation of these data from eq 6, considering the electron stoichiometry of reaction 4. <sup>b</sup> Obtained from results like Figure 5 using plots of eq 6 as in Figure 6.

porphyrin is electrochemically quantitatively reducible,<sup>14a</sup> so the increases in  $\Gamma_T$  are in fact adding larger populations of reduced, active porphyrin catalyst to the electrode surface. Since film thickness presumably also increases with  $\Gamma_T$ , control of the Figure 6 intercepts by diffusion of PhCHBrCH<sub>2</sub>Br in the polymer film (i.e., SUBS flux) seems ruled out by the intercept's lack of response to  $\Gamma_T$ . If the intercept data are analyzed by using eq 6, as done in Table II, the conclusion seems evident that *the substrate reacts with only a fraction of the porphyrin sites*. This conclusion is supported by data derived from Pt/~(Co)(NH<sub>2</sub>)<sub>4</sub>TPP electrocatalysis of this substrate, presented below.

Table II contains results for  $k_{ch}\Gamma$  over the temperature range 20–50 °C which, if plotted as  $\ln [k_{ch}\Gamma]$  vs.  $1/T$  using examples as constant  $\Gamma_T$  (entries 2, 5, 8–10), yield a linear thermal barrier plot with  $E_a = 5.6$  kcal/mol and frequency factor  $Z = 160$  cm/s. That both  $E_a$  and  $Z$  are fairly small is interesting but these results must be considered at best approximate given the scatter in  $k_{ch}\Gamma$  of Table II.

The (in)dependency of  $k_{ch}\Gamma$  on  $\Gamma_T$  was studied further by using the electrocatalytic reduction of 1 mM PhCHBrCH<sub>2</sub>Br solutions by a series of Pt/~(Co)(NH<sub>2</sub>)<sub>4</sub>TPP surfaces which were prepared so as to bear a range of coverages lower than those conveniently prepared with copper, and specifically encompassing values we believe submonomolecular and multimolecular levels. The Koutecky–Levich plots for the Pt/~(Co)(NH<sub>2</sub>)<sub>4</sub>TPP–PhCHBrCH<sub>2</sub>Br reaction are similar to those of Figure 6 and their slopes produce similar results for  $D_S$ , e.g.,  $2.6 \times 10^{-6}$  cm<sup>2</sup>/s. The results for  $k_{ch}\Gamma$  differ slightly according to the cobalt metallation reaction temperature but, as shown in Figure 7, electrodes metallated at 75 and 90 °C display the same general trend. At low coverage,  $k_{ch}\Gamma$  increases with  $\Gamma_T$ , but levels off at ca.  $1 \times 10^{-10}$  mol/cm<sup>2</sup> and becomes relatively independent of  $\Gamma_T$  as was the case for Pt/~(Cu)(NH<sub>2</sub>)<sub>4</sub>TPP surfaces (Table II).

We interpret these results as follows. The reagent Cl<sub>2</sub>Si(CH<sub>3</sub>)(CH<sub>2</sub>)<sub>3</sub>COCl, forming only linear siloxane polymer during the Pt electrode silanization, allows PhCHBrCH<sub>2</sub>Br to readily diffuse through this film to the Pt surface.<sup>28</sup> Incorporation of tetra(*p*-aminophenyl)porphyrin into this film, cross-linking the film by forming an average of two amide bonds per site,<sup>14a</sup> lowers either the partition coefficient ( $P$ ) for PhCHBrCH<sub>2</sub>Br entering the film from the solution or the rate at which PhCHBrCH<sub>2</sub>Br diffuses ( $D_{S,pol}$ ) into (and in) the film, or

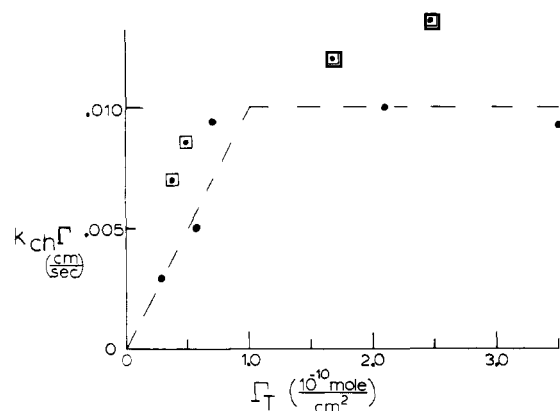


Figure 7.  $k_{ch}\Gamma$  vs.  $\Gamma$  for the reduction of 1 mM PhCHBrCH<sub>2</sub>Br at Pt/~(Co)(NH<sub>2</sub>)<sub>4</sub>TPP electrodes. Me<sub>2</sub>SO/0.1 M TEAP, 20 °C. For each electrode, cobalt was inserted by warming the porphyrin-modified electrode to 75 °C (●) or 90 °C (□) for 6 h in a ~1 M solution of CoCl<sub>2</sub> in DMF. Complete metallation was confirmed by comparing  $\Gamma_T$  measured before and after metal insertion.

both. In the cross-linked film, if the SUBS flux of PhCHBrCH<sub>2</sub>Br which enters the film, and the flux of the chemical reaction, are both less than the CT flux of outwardly migrating reduced porphyrin sites, i.e.,  $D_{ct}C_{TPP} \gg D_{S,pol}PC_S$  and  $D_{ct}C_{TPP}/d \gg k_{ch}\Gamma C_S$ , the above behavior of the Koutecky–Levich  $1/\omega^{1/2} = 0$  intercepts is understandable in that eq 11 reduces to the simple, chemical reaction controlled intercept of eq 6, in which panel A of Figure 4 represents the electrocatalytic reaction profile. In this picture, only the porphyrin sites in the outermost boundary of the film are catalytically operative, and increases in  $\Gamma_T$  beyond completion of this boundary amount of porphyrin yield no dividend in increased catalytic rate.

According to this interpretation, the fold-over coverage in the data of Figure 7 measures the quantity of porphyrin sites present in the outermost boundary or catalytically active zone of the film, i.e., ca.  $1 \times 10^{-10}$  mol/cm<sup>2</sup>. This value is close to that estimated,  $1.2 \times 10^{-10}$  mol/cm<sup>2</sup>, for a coplanar monomolecular level of tetra(*p*-aminophenyl)porphyrin attached to Pt,<sup>14a</sup> which implies then that *the catalytically active zone is approximately one monomolecular layer thick*.

The following support the above interpretation. The coverages  $\Gamma_T$  on Pt/~(Cu)(NH<sub>2</sub>)<sub>4</sub>TPP electrodes in Table II all exceed monomolecular levels and so the constancy of  $k_{ch}\Gamma$  values there is consistent with and expected from the above interpretation. Secondly, in Figure 1, comparison of curves E and F near the foot of the wave shows that current for PhCHBrCH<sub>2</sub>Br reduction is *depressed* at a potential positive of the electrocatalytic wave on a modified surface, supporting the picture of low PhCHBrCH<sub>2</sub>Br flux through the film once porphyrin is bound to it. Thirdly, we observe much lower catalytic rates on Pt/~(Co)(NH<sub>2</sub>)<sub>4</sub>TPP surfaces which are not exhaustively metallated. The free base (NH<sub>2</sub>)<sub>4</sub>TPP sites on such electrodes, being catalytically unstable, become silent, and appear to dilute the active Co(NH<sub>2</sub>)<sub>4</sub>TPP sites and impede substrate access to them. An example is shown in Figure 8, where by comparison of curves A and B only ca. 50% of the original sites are metallated, and, although  $\Gamma_T$  for Co(NH<sub>2</sub>)<sub>4</sub>TPP sites is high ( $3.2 \times 10^{-10}$  mol/cm<sup>2</sup>), a submonomolecular rate,  $k_{ch}\Gamma = 0.002$  cm/s, is observed. Finally, that charge transport through the film is fast compared to the catalytic rate was directly demonstrated by potential step chronoamperometry<sup>29</sup> of a  $1.2 \times 10^{-9}$  mol/cm<sup>2</sup> Pt/

(28) Cyclic voltammetric and chronoamperometric response for PhCHBrCH<sub>2</sub>Br reduction are the same on naked and silanized Pt.

(29) Rocklin, R. D., Ph.D. Thesis, University of North Carolina, Chapel Hill, NC, 1980.

TABLE III: Rotated Disk Electrode Voltammetry Kinetic Results for Electrocatalytic Reductions at 20 °C in 0.1 M Et<sub>4</sub>NClO<sub>4</sub> in Me<sub>2</sub>SO

substrate	$E_{1/2}$ direct V vs. SSCE	$\Gamma_T$ , mol/cm <sup>2</sup>	$C_S$ , mM	$k_{ch}\Gamma$ , <sup>d</sup> cm/s	$k_{ch}$ , L/mol s
Pt/~(Co)(NH <sub>2</sub> ) <sub>4</sub> TPP ( $E^\circ = -0.86$ )					
PhCHBrCHBrPh	-1.36	$2.5 \times 10^{-10}$	1.0	$4.0 \times 10^{-3}$	$4.0 \times 10^4$ <sup>a</sup>
PhCHBrCH <sub>2</sub> Br	-1.45	$2.5 \times 10^{-10}$	1.0	$1.4 \times 10^{-2}$	$1.4 \times 10^5$ <sup>a</sup>
CH <sub>2</sub> BrCHBrCH <sub>3</sub>	-1.89	$2.5 \times 10^{-10}$	4.0	$1.5 \times 10^{-4}$	$1.5 \times 10^3$ <sup>a</sup>
PhCHBrCH <sub>2</sub> Br <sup>b</sup>	-1.45	$0.29 \times 10^{-10}$	1.0	$2.9 \times 10^{-3}$	$1.0 \times 10^5$
		$0.58 \times 10^{-10}$	1.0	$5.0 \times 10^{-3}$	$0.9 \times 10^5$
		$0.71 \times 10^{-10}$	1.0	$9.4 \times 10^{-3}$	$1.3 \times 10^5$
		$2.1 \times 10^{-10}$	1.0	$1.0 \times 10^{-2}$	$1.0 \times 10^5$ <sup>a</sup>
		$3.8 \times 10^{-10}$	1.0	$9.3 \times 10^{-3}$	$0.9 \times 10^5$ <sup>a</sup>
Pt/~(Cu)(NH <sub>2</sub> ) <sub>4</sub> TPP ( $E^\circ = -1.23$ )					
PhCHBrCH <sub>2</sub> Br <sup>c</sup>	-1.45	$4.1 \times 10^{-10}$ - $19 \times 10^{-10}$	1.0	$9.4 \times 10^{-3}$	$0.9 \times 10^5$ <sup>a</sup>

<sup>a</sup> Calculated on basis of active  $\Gamma = 1 \times 10^{-10}$  mol/cm<sup>2</sup>. <sup>b</sup> Data from Figure 7 at 75 °C metallation. <sup>c</sup> Data at 20 °C from Table II, averaged. <sup>d</sup> From plots of data according to eq 6.

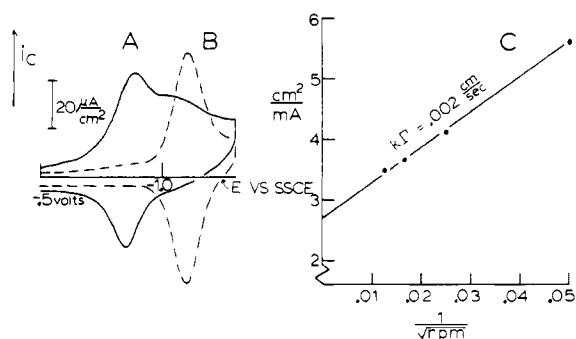


Figure 8. Cyclic voltammetry of Pt/~(Co)(NH<sub>2</sub>)<sub>4</sub>TPP after (curve A) and before (curve B) metallation, in the absence of substrate, in Me<sub>2</sub>SO/0.1 M TEAP,  $\nu = 100$  mV/s, SSCE reference.  $\Gamma_T$ (free base) =  $5.75 \times 10^{-10}$  mol/cm<sup>2</sup>,  $\Gamma_T$ (Co) =  $3.2 \times 10^{-10}$ , indicating incomplete metallation. Curve C: Koutecky–Levich plot for this electrode in 1 mM PhCHBrCH<sub>2</sub>Br, 20 °C. From intercept,  $k_{ch}\Gamma = 2 \times 10^{-3}$  cm/s.

~(NH<sub>2</sub>)<sub>4</sub>TPP electrode, following our previously described approach to measuring  $D_{ct}$ .<sup>20</sup> The film charged very rapidly, >95% in 10 ms, and using  $C_{TPP} = 2 \times 10^{-3}$  mol/cm<sup>3</sup>, only a lower limit for  $D_{ct}$  ( $4 \times 10^{-11}$  cm<sup>2</sup>/s) could be estimated. A film with  $\Gamma_T = 2 \times 10^{-9}$  mol/cm<sup>2</sup> ( $d \approx 10$  nm) and this  $D_{ct}$  should support a CHEM flux of ca.  $8 \times 10^{-8}$  equiv/cm<sup>2</sup> s or a current of 8 mA/cm<sup>2</sup>, which is much larger than the catalytic currents measured in these experiments.

For electrocatalysis by a polymer film with control by the rate of the chemical step, whether the quantity of catalyst sites corresponds to the outermost layer of the film, or to that in the total film ( $\Gamma_T$ ), is predicted by panels A and B of Figure 4 to depend on the ordering of CHEM flux, CT flux, and SUBS flux. In the electrocatalytic reduction of PhCHBrCH<sub>2</sub>Br by Pt/~(Cu)(NH<sub>2</sub>)<sub>4</sub>TPP and Pt/~(Co)(NH<sub>2</sub>)<sub>4</sub>TPP described above, and possibly in the results of Oyama and Anson,<sup>6a</sup> it appears that the quantity of catalyst sites is monolayer-like, corresponding to panel A, Figure 4. In the electrocatalytic results of Lewis et al.,<sup>5a</sup> on the other hand, using a small and slowly reacting substrate (iodide) which should be partitioned into the cationic polymer, SUBS flux is apparently larger and the result is closer to panel B, Figure 4.

Using a single rotated disk Pt/~(Co)(NH<sub>2</sub>)<sub>4</sub>TPP electrode to facilitate comparison of kinetics, we determined  $i_{max}$  for reduction of PhCHBrCH<sub>2</sub>Br, PhCHBrCHBrPh, and CH<sub>2</sub>BrCHBrCH<sub>3</sub> as a function of  $\omega$ , giving Koutecky–Levich plots comparable to Figure 6, and results for  $k_{ch}\Gamma$  which are shown in Table III.  $k_{ch}\Gamma$  was not determined as a function of  $\Gamma_T$  for PhCHBrCHBrPh and

CH<sub>2</sub>BrCHBrCH<sub>3</sub>, so whether the catalytically active zone of a Pt/~(Co)(NH<sub>2</sub>)<sub>4</sub>TPP electrode is the same for these substrates as for PhCHBrCH<sub>2</sub>Br (e.g.,  $1 \times 10^{-10}$  mol/cm<sup>2</sup>) is uncertain. Assuming<sup>30</sup> that it is, we have converted the  $k_{ch}\Gamma$  values for these substrates to  $k_{ch}$  by dividing by the monolayer value  $\Gamma = 1 \times 10^{-10}$  mol/cm<sup>2</sup>. Results of Figure 7 and for Pt/~(Cu)(NH<sub>2</sub>)<sub>4</sub>TPP in Table II, converted to  $k_{ch}$  on the same basis, are also given in Table III, to facilitate their comparison. Values of  $k_{ch}\Gamma$  where  $\Gamma < 1 \times 10^{-10}$  mol/cm<sup>2</sup> in Figure 7 are divided by the actual  $\Gamma$  since complete access is indicated in those cases.

Andrieux et al.<sup>31</sup> have shown, in the homogeneous electrocatalytic reductions of monohaloaromatics with aromatic radical anions, that the RDS involves formation of an ArX<sup>-</sup> that the kinetics slow monotonically in Marcusian fashion as the outer-sphere catalyst couple's  $E^\circ$  become more positive relative to the  $E_{1/2}$  of the ArX reduction wave, and that  $E^\circ$  for the ArX/ArX<sup>-</sup> wave is rather close to the irreversible  $E_{1/2}$ . If the same principles hold for the present case, the catalytic reduction  $k_{ch}$  of PhCHBrCH<sub>2</sub>Br and CH<sub>2</sub>BrCHBrCH<sub>3</sub> by a Pt/~(Cu)(NH<sub>2</sub>)<sub>4</sub>TPP surface should be faster than on Pt/~(Co)(NH<sub>2</sub>)<sub>4</sub>TPP, and with Pt/~(Co)(NH<sub>2</sub>)<sub>4</sub>TPP the order in substrate reduction rate should be PhCHBrCHBrPh > CH<sub>2</sub>BrCHBrCH<sub>3</sub>. Only the final one of these anticipations (slow reduction of CH<sub>2</sub>BrCHBrCH<sub>3</sub> by the Pt/~(Co)(NH<sub>2</sub>)<sub>4</sub>TPP) is actually observed. Catalytic reduction by Pt/~(Co)(NH<sub>2</sub>)<sub>4</sub>TPP is elsewhere faster than expected in comparison with other metalloporphyrins, and the rate order for PhCHBrCHBrPh and PhCHBrCH<sub>2</sub>Br is the reverse of that expected from outer-sphere  $E^\circ$  considerations. The conclusion seems obvious that reductions of these substrates with (Co<sup>I</sup>)(NH<sub>2</sub>)<sub>4</sub>TPP sites do not proceed by an outer-sphere electron transfer pathway and their behavior is not in conflict with the predictions of Andrieux and Saveant<sup>26</sup> as regards outer-sphere electrocatalysis by electrodes with monolayer coverages of catalyst. The reaction must involve adduct formation of some sort, but we have no reasonable basis on which to conjecture about the nature of this binding or the mechanistic details of electron transfer. We should take note, however, of the similarity of the rate for the cobalt and copper porphyrin reactions with PhCHBrCH<sub>2</sub>Br (which may not be fortuitous) and of the greater steric bulkiness of the slower reacting

(30) If this assumption is in error for PhCHBrCHBrPh, the difference in  $k_{ch}$  between PhCHBrCHBrPh and PhCHBrCH<sub>2</sub>Br is enhanced, not reduced.

(31) Andrieux, C. P.; Blocman, C.; Dumas-Bouchiat, J.-M.; Saveant, J. M. *J. Am. Chem. Soc.* 1979, 101, 3431.

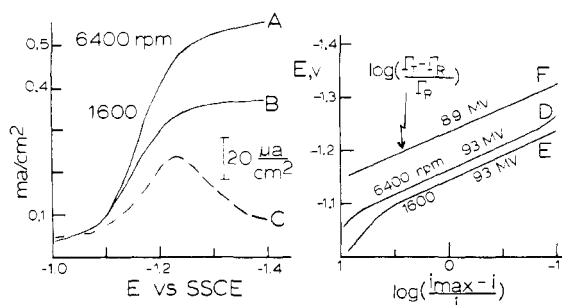


**Figure 9.** Curves A and B: Rotated disk voltammetry for the reduction of 0.68 mM PhCHBrCH<sub>2</sub>Br by a Pt/~(Cu)(NH<sub>2</sub>)<sub>4</sub>TPP electrode, sweep rate = 10 mV/s; curve C: porphyrin electrode without substrate present, showing only cathodic voltammogram,  $\Gamma_T = 5.8 \times 10^{-10}$  mol/cm<sup>2</sup>, 100 mV/s; curves D and E: plots of curves A and B according to eq 13; curve F: plot of curve C according to eq 12.

PhCHBrCHBrPh as compared to PhCHBrCH<sub>2</sub>Br. These facts suggest that the RDS in the reaction could involve steric requirements of adduct formation in the poorly penetrable, catalytically active reaction zone of the porphyrin film.

We consider finally use of the rising portion of the catalytic wave for kinetic measurements. Current-potential curves are shown in Figure 9, curves A and B, for the reduction of PhCHBrCH<sub>2</sub>Br by a Pt/~(Cu)(NH<sub>2</sub>)<sub>4</sub>TPP electrode (entry 5, Table II). The half-wave potential,  $E_{1/2}$  (at  $i = 0.5i_{\max}$ ) becomes more positive, at lower electrode rotation rate, as expected from eq 13. Application of eq 13 to calculation of  $k_{\text{ch}}\Gamma$ , however, yields a value of 0.11 cm/s, in poor agreement with results from  $i_{\max}$  data and Koutecky-Levich plots (Table II). Further, when the catalytic waveshape is analyzed by eq 13, plotting potential vs.  $\log [(i_{\max} - i)/i]$ , the plots (curves D and E) are linear in their central portions but have slopes of 93 mV rather than the 59-mV value expected from eq 13. Equation 13 is thus not a good representation of the rising part of the catalytic wave.

The problem with eq 13 is traceable to the assumption in eq 12 that the activity coefficients of oxidized and reduced porphyrin sites are equal and coverage independent. Electrochemical waves of surface immobilized chemicals in fact show substantial activity effects as pointed out by Brown and Anson and verified elsewhere.<sup>1,14b,32</sup> The surface wave for Pt/~(Cu)(NH<sub>2</sub>)<sub>4</sub>TPP has for example  $E_{\text{whm}} = 145$  mV compared to the 91 mV expected from eq 12. Further, if a plot is made of eq 12 for the Pt/~(Cu)(NH<sub>2</sub>)<sub>4</sub>TPP surface wave (no substrate, Figure 9, curve F), it has the same high slope (89 mV) as the analogous waveshape plot of eq 13 (Figure 9, curve F). Equation 13 fails then, because of neglect of an activity problem.

The activity problem can be circumvented by recognizing that, at any given potential, we can write

$$\frac{\Gamma_T - \Gamma}{\Gamma} = \left[ 1 + \frac{k_{\text{ch}}\Gamma}{0.62D_S^{2/3}\nu^{-1/6}\omega^{1/2}} \right] \left[ \frac{i_{\max} - i}{i} \right] \quad (14)$$

The left-hand side of eq 14 can be evaluated from the Pt/~(Cu)(NH<sub>2</sub>)<sub>4</sub>TPP surface wave so as to explicitly represent the porphyrin activity. If  $k_{\text{ch}}\Gamma$  is evaluated from eq 14, and accounting for the electron stoichiometry of eq 5, a value of 0.019 cm/s results from Figure 9, in much better agreement with the Koutecky-Levich result.

A similar analysis of the rising part of the catalysis for PhCHBrCH<sub>2</sub>Br at a Pt/~(Co)(NH<sub>2</sub>)<sub>4</sub>TPP electrode pro-

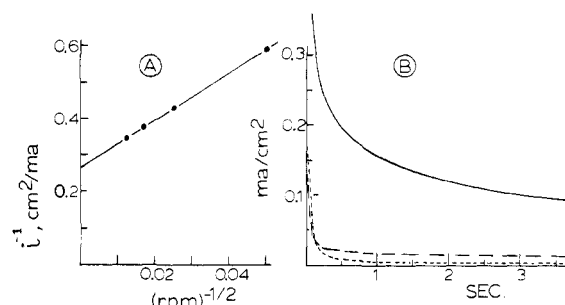


**Figure 10.** Panel A:  $1/i_{\max}$  vs.  $1/\omega^{1/2}$  from rotated disk reduction of 1.17 mM PhCHBrCHBrPh at a Pt/~(Co)(NH<sub>2</sub>)<sub>4</sub>TPP electrode,  $\Gamma_T = 3.3 \times 10^{-10}$  mol/cm<sup>2</sup> in Me<sub>2</sub>SO/0.1 M TEAP, 25 °C. Panel B: Chronoamperometric current time curves at the same electrode in 1.17 mM PhCHBrCHBrPh for a potential step from -0.6 to -1.0 V vs. SSCE reference. The solid line is the catalytic reduction, (---) is the uncatalyzed reduction, and (- - -) is a potential step with the modified electrode in a solution containing no substrate.

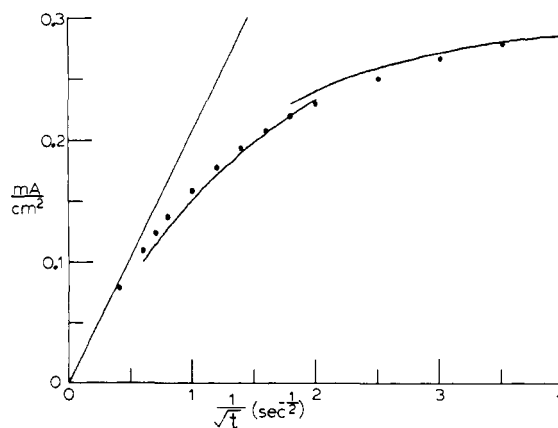


**Figure 11.**  $i$  vs.  $t^{-1/2}$  (solid curve) from the data of Figure 10B plus other data taken at short time (0–0.37 s). The currents are corrected for the background current from a potential step with a modified electrode in a solution containing no substrate. From Figure 10A,  $k_{\text{ch}}\Gamma = 1.66 \times 10^{-3}$  cm/s for this electrode. Points (●) represent theoretical prediction of eq 15 for  $k_{\text{ch}}\Gamma = 1.66 \times 10^{-3}$  cm/s and  $D_S = 2.65 \times 10^{-6}$  cm<sup>2</sup>/s. The linear solid line is a Cottrell slope calculated for  $D_S = 2.65 \times 10^{-6}$  cm<sup>2</sup>/s.

duced via eq 14 a  $k_{\text{ch}}\Gamma$  of 0.015 cm/s as compared to 0.015 cm/s for the Koutecky-Levich plot for this electrode. Nonetheless, the rising part of the current potential curve seems less promising for kinetic measurements than the use of eq 6.

**Chronoamperometry.** Potential step chronoamperometry has not previously been applied to the study of modified electrode electrocatalysis. Its theory is straightforward. Solution of Fick's laws for substrate S under the boundary condition  $D_S(dC_S/dx)_{x=0} = (d\Gamma/dt) = k_{\text{ch}}\Gamma C_S$  yields the current-time equation

$$i = nFAk_{\text{ch}}\Gamma_R C_S \exp \left[ \frac{k_{\text{ch}}\Gamma_R t^{1/2}}{D_S^{1/2}} \right]^2 \operatorname{erfc} \left[ \frac{k_{\text{ch}}\Gamma_R t^{1/2}}{D_S^{1/2}} \right] \quad (15)$$

where  $\Gamma_R = \Gamma$  if the potential step is well onto the plateau of the catalytic wave and  $\Gamma_R = \Gamma / (1 + \exp[(nF/RT)(E^{\circ}_{\text{surf}} - E)])$  if onto the rising portion of the wave. Equation 15 is of the same form as the known relationship for slow charge transfer at naked electrodes<sup>33</sup> where the heterogeneous electron transfer rate constant  $k_{\text{th}}$  is identified with

$k_{\text{ch}}\Gamma$ . The essential difference between the older theory and that for modified electrode electrocatalysis is that  $k_{\text{ch}}$  increases exponentially with potential (and so there is no wave plateau unless mass transfer intervenes) whereas  $k_{\text{ch}}\Gamma_{\text{R}}$  increases with potential only to a maximum value of  $k_{\text{ch}}\Gamma$ . The current-time form of eq 15 can be inspected in several ways;<sup>27</sup> we elected to use plots of  $i$  vs.  $t^{-1/2}$ , a form to which eq 15 linearizes at long time in the experiment, when current becomes limited by the rate of substrate diffusion rather than by the rate of the catalytic reaction.

The chronoamperometric experiment was applied to reduction of PhCHBrCHBrPh with Pt/ $\sim(\text{Co})(\text{NH}_2)_4$ TPP electrodes for which the value of  $k_{\text{ch}}\Gamma$  had been first determined from rotated disk electrode data via a Koutecky-Levich plot. Figure 10A shows such a plot for PhCHBrCHBrPh reduction and Figure 10b shows the current-time curves for a potential step to  $-1.0$  V vs. SSCE at this electrode in a quiet solution of 1.2 mM PhCHBrCHBrPh and in a solution containing no substrate (for background current correction). Figure 11 shows that the current-time response is accurately fit by eq 15 using

a value of  $k_{\text{ch}}\Gamma = 1.66 \times 10^{-3}$  cm/s (the same as obtained from the rotated disk experiment) and a value of  $D_{\text{S}} = 2.65 \times 10^{-6}$  cm<sup>2</sup>/s obtained by a direct potential step reduction (at  $-1.65$  V) of PhCHBrCHBrPh at a naked Pt electrode. A similarly good comparison was obtained in an experiment with a different electrode and 5 mM substrate. The chronoamperometric experiment is simple to apply and this comparison shows that it can be an accurate technique for electrocatalytic measurements. We should note, however, that eq 15 assumes (as does eq 6) fast charge transport through the catalyst film, which may not be the case with other catalyst film systems. Additionally, inclusion of theory for charge transport and substrate diffusion rate effects is a more complex problem than in rotated disk electrode voltammetry, owing to the steady-state character of the latter.

*Acknowledgment.* The research was supported by grants from the Office of Naval Research and by the National Science Foundation. This is part of a series of publications on Chemically Modified Electrodes, no. 31.

## Relaxation Kinetics of Steady States in the Continuous Flow Stirred Tank Reactor. Response to Small and Large Perturbations: Critical Slowing Down

M. Heinrichs and F. W. Schneider\*

*Institute of Physical Chemistry, University of Würzburg, D-8700 Würzburg, West Germany (Received: January 6, 1981; In Final Form: March 19, 1981)*

We present a calculation of relaxation times for a number of reversible reactions whose continuous flow stirred tank reactor (CSTR) steady states have been perturbed by a small perturbation. It is shown that Eigen and DeMaeyer's relaxation expressions at equilibrium are a special case of the corresponding CSTR expressions for which the flow rate is set equal to zero. Of interest are autocatalytic reactions which show the phenomenon of critical slowing down ( $\tau_2 \rightarrow \infty$ ) in the CSTR at the critical flow rate. A comparison with large perturbations is given for which a defined approach time to the steady state is used in place of the relaxation time. This approach time may become infinitely large only for an autocatalytic reaction containing an intermediate species. This is shown for a three-step mechanism which represents the ultimate reduction of our proposed cyclic replication mechanism. The damping effect of an autocatalytic reaction in the CSTR with respect to large perturbations is demonstrated. We show that two independent parallel autocatalytic reactions display *absolute* selectivity of one product over the other if the flow rate is adjusted properly.

### Introduction

Relaxation methods measure the kinetics of reequilibration of a chemical equilibrium that has been perturbed by a small transient or periodic perturbation.<sup>1</sup> They take advantage of a considerable simplification of the differential equations by neglect of higher-order perturbation terms. Thus innumerable rate constants have been determined for a large variety of systems.<sup>1,2</sup> In an analogous fashion to closed equilibrium systems the relaxation technique may be applied to open reactions that are in a steady state. The continuous flow stirred tank reactor (CSTR) is a particularly suitable experimental device for the study of open systems and steady states. The CSTR

is known for its wide use in industrial and chemical engineering<sup>3</sup> as well as in certain biological applications.<sup>3,4</sup> In recent work<sup>5</sup> we have given analytical solutions for the temporal approach of linear networks and nonlinear single-step reactions of any higher order to their steady states (SS) in the CSTR as a consequence of an applied small perturbation. Although the time course of the actual concentrations in the CSTR may become quite complex, the CSTR relaxation times assume relatively simple expressions which may be compared with Eigen and DeMaeyer's relaxation expressions at equilibrium<sup>1</sup> for transient perturbations. Periodic perturbations will be con-

(1) M. Eigen and L. DeMaeyer in "Technique of Organic Chemistry", S. L. Friess, E. S. Lewis, and A. Weissberger, Ed., Vol. VIII, part 2, Wiley-Interscience, New York, 1963.

(2) C. F. Bernasconi, "Relaxation Kinetics", Academic Press, New York, 1976.

(3) L. Lapidus and N. R. Amundson, Eds., "Chemical Reactor Theory. A Review", Prentice-Hall, Englewood Cliffs, NJ, 1977.

(4) F. W. Schneider, D. Neuser, and M. Heinrichs in "Molecular Mechanisms of Biological Recognition", M. Balaban, Ed., Elsevier/North Holland, Biomedical Press 1979, p 241.

(5) M. Heinrichs and F. W. Schneider, *Ber. Bunsenges. Phys. Chem.*, **84**, 857 (1980).